



A Direct Search for New Charged Heavy Leptons at LEP

The OPAL Collaboration

M.Z. Akrawy¹¹, G. Alexander²¹, J. Allison¹⁴, P.P. Allport⁵, K.J. Anderson⁸, J.C. Armitage⁶,
G.T.J. Arnison¹⁸, P. Ashton¹⁴, G. Azuelos¹⁶, J.T.M. Baines¹⁴, A.H. Ball¹⁵, J. Banks¹⁴, G.J. Barker¹¹,
R.J. Barlow¹⁴, J.R. Batley⁵, G. Bavaria¹⁶, F. Beck⁷, K.W. Bell¹⁸, G. Bella²¹, S. Bethke¹⁰, O. Biebel³,
I.J. Bloodworth¹, P. Bock¹⁰, H. Breuer⁷, R.M. Brown¹⁸, R. Brun⁷, A. Buijs⁷, H.J. Burckhart⁷,
P. Capiluppi², R.K. Carnegie⁶, A.A. Carter¹¹, J.R. Carter⁵, C.Y. Chang¹⁵, D.G. Charlton⁷,
J.T.M. Chin¹⁴, I. Cohen²¹, J.E. Conboy¹³, M. Couch¹, M. Coupland¹², M. Cuffiani², S. Dado²⁰,
G.M. Dallavalle¹³, O.W. Davies¹⁴, M.M. Deninno², A. Dieckmann¹⁰, M. Dittmar⁴, M.S. Dixit¹⁷,
D. Duchesneau¹⁶, E. Duchovni²⁴, I.P. Duerdoth^{7,c}, D. Dumas⁶, H. El Mamouni¹⁶, P.A. Elcombe⁵,
P.G. Estabrooks⁶, E. Etzion²¹, F. Fabbri², P. Farthouat¹⁹, H.M. Fischer³, D.G. Fong¹⁵, M.T. French¹⁸,
C. Fukunaga²², B. Gandois¹⁹, O. Ganel²⁴, J.W. Gary¹⁰, N.I. Geddes¹⁸, C.N.P. Gee¹⁸,
C. Geich-Gimbel³, S.W. Gensler⁸, F.X. Gentil¹⁹, G. Giacomelli², W.R. Gibson¹¹, J.D. Gillies¹⁸,
J. Goldberg²⁰, M.J. Goodrick⁵, W. Gorn⁴, D. Granite²⁰, E. Gross²⁴, P. Grosse-Wiesmann⁷,
J. Grunhaus²¹, H. Hagedorn⁹, J. Hagemann⁷, M. Hansroul⁷, C.K. Hargrove¹⁷, J. Hart⁵,
P.M. Hattersley¹, D. Hatzifotiadou⁷, M. Hauschild⁷, C.M. Hawkes⁷, E. Heflin⁴, J. Heintze¹⁰,
R.J. Hemingway⁶, R.D. Heuer⁷, J.C. Hill⁵, S.J. Hillier¹, P.S. Hinde¹⁴, C. Ho⁴, J.D. Hobbs⁸,
P.R. Hobson²³, D. Hochman²⁴, B. Holl⁷, R.J. Homer¹, S.R. Hou¹⁵, C.P. Howarth¹³,
R.E. Hughes-Jones¹⁴, P. Igo-Kemenes¹⁰, M. Imori²², D.C. Imrie²³, A. Jawahery¹⁵, P.W. Jeffreys¹⁸,
H. Jeremie¹⁶, M. Jimack⁷, E. Jin^{4,b}, M. Jobs¹, R.W.L. Jones¹¹, P. Jovanovic¹, D. Karlen⁶,
K. Kawagoe²², T. Kawamoto²², R.G. Kellogg¹⁵, B.W. Kennedy¹³, C. Kleinwort⁷, D.E. Klem¹⁷,
G. Knop³, T. Kobayashi²², L. Köpke⁷, T.P. Kokott³, M. Koshiba²², R. Kowalewski⁶, H. Kreuzmann³,
J. von Krogh¹⁰, J. Kroll⁸, P. Kyberd¹¹, G.D. Lafferty¹⁴, F. Lamarche¹⁶, W.J. Larson⁴,
M.M.B. Lasota¹¹, J.G. Layter⁴, P. Le Du¹⁹, P. Leblanc¹⁶, D. Lellouch⁷, P. Lennert¹⁰, L. Lessard¹⁶,
L. Levinson²⁴, S.L. Lloyd¹¹, F.K. Loebinger¹⁴, J.M. Lorah¹⁵, B. Lorazo¹⁶, M.J. Losty¹⁷, J. Ludwig⁹,
J. Ma^{4,b}, A.A. Macbeth¹⁴, M. Mannelli⁷, S. Marcellini², G. Maringer³, J.P. Martin¹⁶, T. Mashimo²²,
P. Mättig⁷, U. Maur³, T.J. McMahon¹, A.C. McPherson⁶, F. Meijers⁷, D. Menszner¹⁰, F.S. Merritt⁸,
H. Mes¹⁷, A. Michelini⁷, R.P. Middleton¹⁸, G. Mikenberg²⁴, D.J. Miller¹³, C. Milstene²¹, M. Minowa²²,
W. Mohr⁹, A. Montanari², T. Mori²², M.W. Moss¹⁴, A. Muller¹⁹, P.G. Murphy¹⁴, W.J. Murray⁵,
B. Nellen³, H.H. Nguyen⁸, M. Nozaki²², A.J.P. O'Dowd¹⁴, S.W. O'Neale^{7,d}, B. O'Neill⁴,
F.G. Oakham¹⁷, F. Odoricci², M. Ogg⁶, H. Oh⁴, M.J. Oreglia⁸, S. Orito²², G.N. Patrick¹⁸,
S.J. Pawley¹⁴, J.E. Pilcher⁸, J.L. Pinfold²⁴, D.E. Plane⁷, B. Poli², A. Possoz^{8,e}, A. Pouladdeji⁶,
T.W. Pritchard¹¹, G. Quast⁷, J. Raab⁷, M.W. Redmond⁸, D.L. Rees¹, M. Regimbald¹⁶, K. Riles⁴,
C.M. Roach⁵, F. Roehner⁹, A. Rollnik³, J.M. Roney⁸, A.M. Rossi^{2,a}, P. Routenburg⁶, K. Runge⁹,
O. Runolfsson⁷, S. Sanghera⁶, R.A. Sansum¹⁸, M. Sasaki²², B.J. Saunders¹⁸, A.D. Schaile⁹,
O. Schaile⁹, W. Schappert⁶, P. Scharff-Hansen⁷, H. von der Schmitt¹⁰, S. Schreiber³, J. Schwarz⁹,

A. Shapira²⁴, B.C. Shen⁴, P. Sherwood¹³, A. Simon³, G.P. Siroti², A. Skuja¹⁵, A.M. Smith⁷, T.J. Smith¹, G.A. Snow¹⁵, E.J. Spreadbury¹³, R.W. Springer¹⁵, M. Sproston¹⁸, K. Stephens¹⁴, J. Steuerer⁹, H.E. Stier⁹, R. Ströhmer¹⁰, D. Strom⁸, H. Takeda²², T. Takeshita²², T. Tsukamoto²², M.F. Turner⁵, G. Tysarczyk¹⁰, D. Van den plas¹⁶, G.J. VanDalen⁴, C.J. Virtue¹⁷, A. Wagner¹⁰, C. Wahl⁹, H. Wang^{4,b}, C.P. Ward⁵, D.R. Ward⁵, J. Waterhouse⁶, P.M. Watkins¹, A.T. Watson¹, N.K. Watson¹, M. Weber¹⁰, S. Weisz⁷, N. Wermes⁷, M. Weymann⁹, G.W. Wilson⁷, J.A. Wilson¹, I. Wingerter⁷, V.H. Winterer⁹, N.C. Wood¹³, S. Wotton⁷, B. Wuensch³, T.R. Wyatt¹⁴, R. Yaari²⁴, H. Yamashita²², Y. Yang^{4,b}, G. Yekutieli²⁴, W. Zeuner⁷, G.T. Zorn¹⁵, S. Zylberajch¹⁹.

¹School of Physics and Space Research, University of Birmingham, Birmingham, B15 2TT, UK

²Dipartimento di Fisica dell' Università di Bologna and INFN, Bologna, 40126, Italy

³Universität Bonn, D-5300 Bonn 1, FRG

⁴Department of Physics, University of California, Riverside, CA 92521 USA

⁵Cavendish Laboratory, Cambridge, CB3 0HE, UK

⁶Carleton University, Dept of Physics, Colonel By Drive, Ottawa, Ontario K1S 5B6, Canada

⁷CERN, European Organisation for Particle Physics, 1211 Geneva 23, Switzerland

⁸Enrico Fermi Institute and Dept of Physics, University of Chicago, Chicago Illinois 60637, USA

⁹Fakultät für Physik, Albert Ludwigs Universität, D-7800 Freiburg, FRG

¹⁰Physikalisches Institut, Universität Heidelberg, D-6900 Heidelberg, FRG

¹¹Queen Mary and Westfield College, University of London, London, E1 4NS, UK

¹²Birkbeck College, London, WC1E 7HV, UK

¹³University College London, London, WC1E 6BT, UK

¹⁴Department of Physics, Schuster Laboratory, The University, Manchester M13 9PL, UK

¹⁵Dept. of Physics and Astronomy, University of Maryland, College Park, Maryland 20742, USA

¹⁶Laboratoire de Physique Nucleaire, Université de Montreal, Montreal, Quebec, H3C 3J7, Canada

¹⁷National Research Council, Herzberg Institute of Astrophysics, Ottawa, Ont. K1A 0R6, Canada

¹⁸Rutherford Appleton Laboratory, Chilton, Didcot, Oxfordshire, OX11 0QX, UK

¹⁹DPhPE, CEN Saclay, F-91191 Gif-sur-Yvette France

²⁰Department of Physics, Technion-Israel Institute of Technology, Haifa 32000, Israel

²¹Department of Physics and Astronomy, Tel Aviv University, Tel Aviv 69978, Israel

²²Int. Center for Elementary Particle Phys. and Dept. of Phys., Univ. of Tokyo, Tokyo 113, and Kobe University, Kobe 657, Japan

²³Brunel University, Uxbridge, Middlesex, UB8 3PH, UK

²⁴Nuclear Physics Department, Weizmann Institute of Science, Rehovot, 76100, Israel

^aPresent address: Dipartimento di Fisica, Università della Calabria, 87036 Rende, Italy

^bOn leave from Harbin Institute of Technology, Harbin, China

^cOn leave from Manchester University

^dOn leave from Birmingham University

^ePresent address: EPFL, Lausanne

(Submitted to Physics Letters)

Abstract

Results are presented from a search for a new charged heavy lepton in e^+e^- annihilation. The data were taken with the OPAL detector at LEP during a scan of the Z^0 resonance. Two independent search techniques were used, one looking for events with large missing energy and missing momentum transverse to the beam, and the other for events with isolated energetic leptons. Two candidate events, consistent with expected background, were found in the first search; none was found in the second. These results allow the exclusion at the 95% confidence level of a charged heavy lepton of mass less than $44.3 \text{ GeV}/c^2$ if it is assumed to have a massless neutrino partner. Limits are also presented for the case of a massive neutrino.

1 Introduction

This paper presents a search for a fourth-generation charged heavy lepton L produced in e^+e^- collisions on the Z^0 resonance at LEP. In this analysis we assume that the charged heavy lepton decays via the standard charged current coupling into an associated stable neutrino ν_L . Previous searches at other accelerators have set experimental limits on such a particle of $m_L > 30$ GeV/ c^2 at 95% CL from e^+e^- collisions[1] and $m_L > 41$ GeV/ c^2 at 90% CL from $p\bar{p}$ collisions [2] assuming that the associated neutrino ν_L is massless. In this paper we obtain improved limits on m_L for the case of a massless neutrino ($m_{\nu_L} = 0$) as well as for the more general case $0 < m_{\nu_L} < m_L$. LEP provides a good environment in which to pursue these searches because of the high energy, high luminosity, and low backgrounds.

The Z^0 is assumed to couple to L^+L^- in the same way that it couples to lighter leptons. The lowest-order production cross-section is given [3] by:

$$\begin{aligned} \sigma_{e^+e^- \rightarrow L^+L^-} = & \frac{4\pi\alpha^2}{3s} \beta \frac{(3-\beta^2)}{2} \left\{ 1 + \frac{(1-4\sin^2\theta_W)^2}{8\sin^2\theta_W\cos^2\theta_W} \frac{s(s-M_Z^2)}{(s-M_Z^2)^2 + M_Z^2\Gamma_Z^2} \right. \\ & \left. + \frac{(1-4\sin^2\theta_W)^2 + 1}{256\sin^4\theta_W\cos^4\theta_W} \left[(1-4\sin^2\theta_W)^2 + \frac{2\beta^2}{3-\beta^2} \right] \frac{s^2}{(s-M_Z^2)^2 + M_Z^2\Gamma_Z^2} \right\} \end{aligned}$$

where s is the square of the center-of-mass energy, M_Z and Γ_Z are the mass and width of the Z^0 boson, θ_W is the weak mixing angle, and β is the velocity of the heavy leptons in the final state:

$$\beta \equiv \sqrt{1 - \frac{4M_L^2}{s}}$$

Higher-order radiative corrections substantially reduce this cross section on and below the Z^0 resonance. The production cross-section depends sensitively on M_L through β ; for example, if $M_L = 44$ GeV/ c^2 , then for the integrated luminosities presented below we expect 785 $\mu^+\mu^-$ pairs to be produced, but only 17.4 L^+L^- pairs.

Ignoring small corrections, the branching ratios for the leptonic decays $L \rightarrow \nu_L + l + \nu_l$ ($l = e, \mu, \tau$) are each $\frac{1}{9}$, and the branching ratio for semi-leptonic decays $L \rightarrow \nu_L + \text{hadrons}$ is $\frac{2}{3}$. Including the tau leptonic decays ($\tau \rightarrow e\nu_e\nu_\tau, \mu\nu_\mu\nu_\tau$) gives a total branching ratio to e or μ of 26%, and consequently 45% of L^+L^- pairs are expected to decay into a system containing at least one isolated energetic electron or muon. All heavy lepton events contain at least two energetic neutrinos, which result in large missing energy and missing transverse momentum.

We have carried out two different searches for L using independent signatures: (1) missing energy and missing momentum transverse to the beam direction, and (2) an isolated high-momentum e or μ . The first search is sensitive to both the semi-leptonic and leptonic decays of a heavy lepton, and the second is sensitive only to events with at least one leptonic decay.

2 Monte Carlo Generation

Heavy lepton production was simulated with the TIPTOP [4] Monte Carlo program, which includes mass effects, initial-state radiative corrections and spin-spin correlations among heavy lepton decay products. The LULEPT [5] Monte Carlo program was also used as a check of systematic errors

in production simulation. Radiative corrections in these Monte Carlo programs include only first-order effects [6], which tend to underestimate heavy lepton production cross sections. An additional, approximate correction was applied to calculated cross sections based on a second-order treatment of radiation with exponentiation of soft photons. [7]

In calculating expected numbers of events for heavy leptons of various masses, the variation of cross sections with the different center-of-mass energies at which the data were recorded must be taken into account. In the cross-section calculations, we have used our previously measured values [8] of the Z^0 mass and width. Luminosities were derived from measuring the rate of low-angle Bhabha scattering events in the forward calorimeter; the systematic error on the measured integrated luminosity is estimated to be 5%. Table 1 shows the total number of events expected for various heavy lepton masses for the different center-of-mass energies contributing to this analysis.

3 The Detector

The data were recorded with the OPAL detector [9] at the CERN e^+e^- collider, LEP, during the collider's first two months of operation, and correspond to an integrated luminosity of 752 nb^{-1} . OPAL is a multipurpose apparatus designed to measure the decay products of the Z^0 boson. The detector contains a system of central drift chambers inside a 0.435 Tesla solenoidal magnetic field; these include a precision vertex chamber, a large-volume central "jet chamber" which gives precision tracking in the r - ϕ plane, and chambers for tracking in the r - z plane. The most important tracking element for this analysis is the jet chamber, which is four meters in length and two meters in radius, containing 159 layers of sense wires in 24 azimuthal sectors. The solenoid is surrounded by a time-of-flight (TOF) scintillating-counter array, a lead glass electromagnetic calorimeter with a presampler, an instrumented magnet return yoke serving as a hadron calorimeter, and four layers of muon chambers. Similar calorimetry and muon chambers cover the two endcaps of the detector. The electromagnetic calorimeter consists of a cylindrical array of 9,440 lead-glass blocks, each 10 cm x 10 cm in cross-section with 24.6 radiation lengths thickness and oriented to point approximately toward the interaction point, and an endcap of 2,264 lead glass blocks with 20.0 radiation lengths thickness, each pointing along the beam direction. A small-angle calorimeter, called the forward detector (FD), serves as a luminosity monitor. The components of the OPAL detector are described in more detail elsewhere [9] [10].

The triggers used in this analysis are based on four independent detector components: the electromagnetic calorimeter, the time-of-flight system (TOF), the jet chamber, and the barrel muon chambers. The calorimeter trigger requires an energy sum of at least 6 GeV in the lead-glass barrel or in one endcap, and the TOF trigger requires hits in at least three nonadjacent time-of-flight counters. A track trigger for charged particles requires that at least two jet-chamber tracks must originate from the vertex in the r - z projection with a minimum transverse momentum of 450 MeV/c each. In addition, an event is recorded if a track found in the muon barrel chambers (with three out of four planes) is associated within 260 mrad in azimuth with either a signal in a TOF scintillator or a track found in the central detector. The calorimeter, TOF, and track triggers are independent, which allows a cross-check of trigger efficiencies.

All events were passed through an on-line event filter [10] to reject trivial backgrounds. For events passing the selections described below, the combined trigger and filter selection efficiencies were determined from Monte Carlo studies to be greater than 98% for heavy leptons with massless neutrinos.

4 Event Selection

In each of the two searches, some common event selection criteria were applied. Data were rejected when the jet-chamber voltage and the magnetic field were not at nominal operating values. Backgrounds from cosmic rays and beam-gas interactions were suppressed by requiring each event to have at least one reconstructed jet-chamber track with measured $d_0 < 0.5$ cm, $z_0 < 40$ cm, and $p_{\perp} > 150$ MeV/c; p_{\perp} is the momentum of the track in the plane transverse to the beam, d_0 is the distance of closest approach of the track to the beam axis, and z_0 is the longitudinal displacement from the nominal interaction point at the point of closest approach to the beam. Remaining cosmic-ray events were suppressed by requiring at least one time signal from the TOF counters to be between 2 and 12 ns after the beam crossing.

Both searches used tracks reconstructed in the central jet chamber and electromagnetic clusters found in the lead-glass calorimeter. To ensure accurate track reconstruction for accepted events, each track used in the analysis was required to have $d_0 < 1$ cm and $z_0 < 80$ cm, at least 30 associated wire hits in the jet chamber, a transverse momentum $p_{\perp} > 150$ MeV/c, and an angle of at least 170 mrad in the polar angle θ (the angle between the track direction and the beam axis). All events were required to have at least two tracks satisfying these criteria. Electromagnetic clusters were defined by a set of one or more contiguous lead glass blocks, each with at least 20 MeV energy. Clusters used in this analysis were required to have at least 100 MeV energy in the barrel calorimeter, and at least 200 MeV in the endcaps. Tracks were associated with clusters if the extrapolated track and the cluster matched to within 50 mrad in azimuthal angle and 150 mrad in polar angle.

The first search is based on the total visible energy in the event and on the component of the total momentum transverse to the beam direction. These two quantities are calculated by summing the four-momenta derived from each accepted track in the jet chamber and from each cluster in the lead-glass electromagnetic calorimeter, assuming massless particles. If a cluster has one or more tracks associated to it, only the excess of the cluster energy over the total associated track energy is included in the sum (this is to avoid double-counting of energy). The four-momentum sum is used to define the total visible energy E_{vis} , the magnitude p_t of the total momentum transverse to the beam, and the direction of the missing momentum.

In Figure 1, the distributions of measured E_{vis} and p_t for a sample of hadronic Z^0 decays are compared with Monte-Carlo Z^0 events [11] whose reconstruction includes a detailed simulation of the OPAL detector. The selection criteria for these multi-hadron events are described in reference [8]. The E_{vis} distributions of both data and Monte-Carlo peak below the Z^0 mass; this downward shift occurs primarily because hadrons produce a smaller signal than electrons in the lead glass calorimeter. Aside from a 5% difference in the peak energies, the data and Monte-Carlo agree well in magnitude, resolution, and in the shapes of both the E_{vis} and p_t distributions.

Because all heavy-lepton events contain at least two final-state neutrinos, heavy lepton candidates are required to have a measured $p_t \geq 12.0$ GeV/c and a visible energy in the range $5.0 \text{ GeV} \leq E_{vis} \leq 55.0 \text{ GeV}$. To suppress background from events with undetected energetic particles escaping down the beam pipe, events are rejected if the energy measured in the forward detector exceeds 5.0 GeV. These cuts reduce the data sample from 22,687 to 315 events, but retain about 50% of heavy-lepton events according to Monte-Carlo calculations (see table 2). The number of observed events is compatible with the numbers of events expected from $Z^0 \rightarrow \tau^+ \tau^-$ (204 ± 13) and $Z^0 \rightarrow \text{hadrons}$ (80 ± 15).

Background from τ -pair production is eliminated by requiring the thrust of the event (calculated from charged tracks alone) to be less than 0.95. This cut rejects virtually all of the τ -pairs but has a small effect on the efficiency for detecting heavy leptons. The data sample is reduced to 47 events by

these cuts, while the acceptance for heavy leptons is only reduced to about 47%.

The remaining background comes primarily from hadronic events in which a mismeasurement of the energy of a jet leads to an artificial missing momentum. This missing momentum tends to lie along the direction of other particles detected in the event. Because of the large heavy lepton mass, the neutrino from the L decay tends not to lie along the directions of other particles. Therefore, we require that there be no energetic detected particles produced in the direction of the missing momentum. We calculate the total energy of charged tracks and electromagnetic clusters within a cone of 30° half-angle around the direction of the missing momentum, and require both of these cone energies E_{cone} to be less than 1 GeV.

Figure 2(a) shows the distribution of E_{vis} vs p_t for the data, after the cuts on thrust and E_{cone} have been applied. Figure 2(b) shows the same distribution expected for a $42 \text{ GeV}/c^2$ charged heavy-lepton (unnormalized). The events at large E_{vis} are multihadronic Z^0 decays; the events at low E_{vis} and low p_t are two-photon events. The signal region defined by the cuts in p_t and E_{vis} is well separated from these backgrounds.

Two events remain, after all of the cuts. The first is a 3-jet multihadron event with two poorly measured jets at low angles, and a third jet in the transverse direction. The second event is a radiative Bhabha event in which one of the electrons has a badly mismeasured momentum due to tracking errors, which give an artificially large p_t . Both of these events lie very close to the boundary of the search region in Figure 2(a). For a heavy lepton of $44 \text{ GeV}/c^2$, we calculate an efficiency after all cuts of 44% and would expect to observe a mean of 7.6 events. The mass limit obtained from this analysis is given below.

The second search is based on the identification of an isolated electron or muon. Only tracks with reconstructed momentum greater than $5 \text{ GeV}/c$ and with $|\cos \theta| \leq 0.7$ are considered as lepton candidates. The track must be associated with a cluster of at least 100 MeV energy in the electromagnetic calorimeter. A minimum-ionizing particle typically produces a signal equivalent to 700 MeV in the electromagnetic calorimeter. The isolation requirement is imposed by requiring that within a cone of 30° half-angle around the isolated track (1) the total energy from other charged tracks be less than 1 GeV, and (2) the total energy of electromagnetic clusters, excluding the cluster associated with the track, be less than 2 GeV. These cuts select 2063 events (see Table 3).

The isolated track must satisfy either the electron selection criteria or the muon selection criteria described below. For electron candidates, the track is required to be associated with an electromagnetic cluster of at least 5 GeV. Backgrounds to the electron signal are isolated charged hadrons with and without overlapping electromagnetic showers. In general, these backgrounds have (1) larger average shower widths than electrons, (2) associated energy penetrating into the hadronic calorimeter, and (3) mismatch between the measured momentum of the track and the measured energy of the cluster. To suppress these backgrounds, electron candidates are required to have electromagnetic clusters of no more than 18 lead-glass blocks, with 90% of the energy contained in no more than 4 blocks. Candidates are rejected if signals are produced in more than 2 planes of the hadron calorimeter within the 30° search cone around the track. Finally, there must be approximate agreement between the measured momentum p of the track and the measured electromagnetic energy E of the associated cluster. One of the following two conditions must be met:

$$0.50 \leq \frac{p}{E} \leq 1.2,$$

$$-3 \leq \frac{1/p - 1/E}{\sigma_{inv}} \leq 3,$$

where σ_{inv} is the quadrature sum of the calculated errors on $1/p$ and $1/E$. The first condition allows for radiation by the electron, either at the event vertex or in traversing material in the detector. The second condition is important only at the highest momenta, where the error in $1/p$ is large.

For muon candidates, the number of lead-glass blocks in the associated electromagnetic cluster is required to be no more than 4. In addition, penetration to the outer layers of the detector is required. There must be an associated signal in at least 2 of the outer 7 planes consisting of the last 3 hadron calorimeter layers and the 4 muon chamber layers. Finally, the total electromagnetic energy within the 30° search cone must be less than 5 GeV.

The isolated lepton requirement selects 1388 events, the great majority of which are conventional dileptons (e^+e^- , $\mu^+\mu^-$, $\tau^+\tau^-$). These are easily recognized, since they typically have back-to-back single tracks (in the case of $e^+e^- \rightarrow e^+e^-$ and $e^+e^- \rightarrow \mu^+\mu^-$) or narrow back-to-back jets with low invariant mass (in the case of $e^+e^- \rightarrow \tau^+\tau^-$). To identify these, we divide the event into two hemispheres defined by the plane perpendicular to the direction of the isolated lepton. Within each hemisphere, the transverse mass M_h (defined using only the momentum components in the $r-\phi$ plane) is required to be less than $2.0 \text{ GeV}/c^2$. In addition, the acolinearity angle θ_{acol} between the total momentum vectors of the two hemispheres is required to be less than 250 mrad. In computing the four-momentum in each hemisphere, both tracks and electromagnetic clusters were used, with double-counting avoided in the manner described previously. In the calculation of mass, however, only tracks were used, since radiative photons can give a spuriously large mass for $e^+e^- \rightarrow e^+e^-$ and $e^+e^- \rightarrow \mu^+\mu^-$ events. The transverse mass was used rather than invariant mass because the resolution in azimuthal angle of the tracks in the central drift chamber is substantially better than that in polar angle.

Any event satisfying all three of these conditions ($\theta_{acol} < 250 \text{ mrad}$, $M_{h1} < 2 \text{ GeV}/c^2$, $M_{h2} < 2 \text{ GeV}/c^2$) is classified as a conventional dilepton and removed from the sample. Although this cut removes 94% of the events in the data sample, the effect on heavy lepton detection efficiency is negligible ($< 1\%$ loss). Figure 3(a) shows the distributions, before the conventional dilepton cut is applied, of the maximum of M_{h1} and M_{h2} for isolated lepton events in the data and for those from a heavy lepton of mass $42 \text{ GeV}/c^2$; figure 3(b) compares the distributions of the θ_{acol} for the same events.

By comparing the events classified as conventional lepton pairs with independently selected samples of $e^+e^- \rightarrow e^+e^-$ and $e^+e^- \rightarrow \mu^+\mu^-$ events, we measure the efficiency for identifying electrons to be $86 \pm 3\%$ and the efficiency for identifying muons to be $92 \pm 3\%$; both of these efficiencies were constant over the running period and are expected to be insensitive to lepton energy (this has been qualitatively verified from a small sample of $e^+e^- \rightarrow e^+e^-\gamma$ events found in the data). From Monte Carlo studies, we expect to find 251 ± 26 $e^+e^- \rightarrow \tau^+\tau^-$ events in this sample of dileptons. After removing identified $e^+e^- \rightarrow e^+e^-$ and $e^+e^- \rightarrow \mu^+\mu^-$ events and correcting for expected residual contamination, we observe 275 ± 8 τ -pairs. This comparison provides a check of our efficiency for detecting heavy leptons, since the energy spectra of electrons and muons in heavy lepton events (if the associated neutrino is massless) should be quite similar to those in τ -pair events.

After the conventional dileptons have been removed, 84 events remain in the data sample. All of these have been examined and appear consistent with expected backgrounds. None suggests a heavy-lepton origin; only 6 are multihadron events. Most of the events appear to be due to either dilepton production with initial state radiation or to dilepton production by two-photon processes. Both of these backgrounds give acolinear dileptons, since they have a large missing momentum due to the undetected particles which escape down the beam pipe. Twelve of these events show substantial energy in the forward detector, indicating that a small-angle radiative particle has missed the main

calorimeter. These events are removed by rejecting all events in which the forward detector registers more than 5.0 GeV of energy. For radiative events in which the radiated particles remain within the beam pipe and consequently carry little transverse momentum, the transverse momentum vectors of the detected particles should appear colinear even though their total momentum vectors will not be colinear. Such events can be distinguished from heavy lepton production by their acoplanarity θ_{acop} , defined as the angle between the transverse projections of the total momentum vectors in the two hemispheres (where the two hemispheres are separated by a plane perpendicular to the transverse projection of the isolated lepton). Heavy lepton events tend to have large acoplanarity due to the transverse momentum of the final-state neutrinos. Events with no energetic particles other than the isolated lepton may also be acoplanar, since a small p_t imbalance in such an event can produce a large-angle deflection. Examples are very low-energy two-photon events and highly asymmetric tau decays in which almost all of the energy of one tau goes into final-state neutrinos. These backgrounds are suppressed by requiring that heavy lepton candidates have at least one track in the final state (in addition to the isolated lepton) with an energy E_2 of more than 2 GeV, that there be at least 6 GeV of missing p_t in the event, and that θ_{acop} be greater than 200 mrad. The effect of these cuts is shown in Table 3. The p_t and θ_{acop} distributions of the data are compared with those expected for a heavy lepton in Figure 4.

From Monte Carlo simulation we expect at this stage 0.8 ± 0.8 background events from $\tau^+\tau^-\gamma$, and 0.5 ± 0.5 events from two-photon processes [12]. We observe 1 event, which is consistent with being $\tau^+\tau^-\gamma$ with the γ converting to produce an e^+e^- pair. Final states of this type, where the γ carries significant p_t and is seen in the detector, can be energetic and also acoplanar since they have two energetic non-colinear neutrinos from the τ decays. In general, states of the type $\ell^+\ell^-\gamma$ can be identified by their distinctive topology. The final state contains three particles that must lie in a plane, the energies of which can be calculated from the beam energy and the measured angles between the particles. To remove this background, we discard any event satisfying both of the following conditions: (1) there are exactly three narrow clusters of particles, where two of the clusters each have a net charge of ± 1 and the third one contains either no charged particles or a low-mass pair of oppositely charged particles, consistent with an electron-positron pair from photon conversion; (2) the measured electromagnetic energy of the third cluster agrees within 10% of the expected energy calculated from the cluster directions, assuming these directions to be those of the primary leptons. We have identified more than 30 such states in the dilepton sample, including 19 $e^+e^-\gamma$'s.

After we reject $\ell^+\ell^-\gamma$ states, no events are left in the data sample. The efficiency for detecting heavy lepton events is not changed by this cut. A 44 GeV/ c^2 heavy lepton is expected to produce 3.8 events passing all of our requirements.

5 Limits on Heavy Lepton Masses

The sensitivity of this search for heavy leptons of a given mass can be calculated from the predicted number of produced L^+L^- pairs (table 1) and a Monte-Carlo calculation of the search efficiency. In the case of a massless ν_L , we obtain 95% confidence level limits of $m_L > 44.1$ GeV/ c^2 from the missing p_t search alone, $m_L > 44.2$ GeV/ c^2 from the isolated lepton search alone, and $m_L > 44.3$ GeV/ c^2 from the combined searches; systematic error have been taken into account in the manner described below.

If the ν_L has a non-zero mass, then the production cross-section for L^+L^- of a given mass is unchanged, but the detection efficiencies of the searches are affected. The expected numbers of events found by each of our searches are tabulated for various values of m_L and m_{ν_L} in Table 4. The large

reduction in efficiency for $m_{\nu L} > m_L/2$ occurs because the ν_L necessarily takes most of the energy from the L^\pm decay. This suppresses the rate of production of high-energy e 's and μ 's and of events with large missing p_t , and consequently the acceptance of our selections is reduced and possible systematic errors (e.g., in calibration and resolution) become more important.

We estimate a 5% systematic error from luminosity, a 5% error from lepton identification uncertainty, and typically a 5% error from Monte-Carlo statistics, giving a combined error of about 9%. In addition, to allow for possible differences between the data and Monte-Carlo, we have varied the p_t cut in the missing p_t search by $\pm 10\%$, the lepton momentum cut in the isolated lepton search by $\pm 10\%$, and the cuts on cone energy in both searches by $\pm 100\%$. The variation in selection efficiencies within these ranges is used as a measure of systematic error, and is added in quadrature with the other errors. In setting 95% C.L. limits on the masses of the leptons, we have reduced the number of events predicted at each point by one sigma before calculating the Poisson 95% confidence level contour. The C.L. limits are sensitive to this systematic error only in the region of highest $m_{\nu L}$, where the effect is still less than $0.8 \text{ GeV}/c^2$ in $m_{\nu L}$. The resulting C.L. contour is shown in Figure 5.

We have chosen to apply fixed boundaries to the contour along the lines $m_L - m_{\nu L} = 5 \text{ GeV}/c^2$ and $m_L - m_{\nu L} = 0.25m_L$ because our selection efficiency is low above this line, and this region is better studied through other kinds of searches. In the region $m_L < 38 \text{ GeV}/c^2$, the number of events predicted at any point in the shaded region is always at least twice that required for 95% C.L. limits; this includes the boundary, where rates are lowest. In the high-mass region, $m_L > 41 \text{ GeV}/c^2$, the efficiency is always at least 10% for the missing p_t search and always at least 5% for the isolated lepton search ($\geq 17\%$ for leptonic decay modes within $\cos(\theta) < 0.70$); the limits here are governed primarily by the steeply falling production cross-section of L^+L^- events. Within the shaded region, our trigger efficiency has been determined from Monte-Carlo studies to be greater than 96% at all points for events passing our selection cuts.

In summary, in each of two searches we find no evidence for a new charged heavy lepton being produced in the decays of the Z^0 boson. A charged heavy lepton is excluded at 95% confidence level for masses below $44.3 \text{ GeV}/c^2$ with $m_{\nu L} < 20 \text{ GeV}/c^2$. For ν_L with higher mass, we exclude at 95% confidence level the shaded region of Figure 5, approximately defined by $m_L < 43 \text{ GeV}/c^2$, $m_{\nu L} < 30 \text{ GeV}/c^2$, and $m_{\nu L} < 0.75m_L$. These results are consistent with those of another experimental study, based on a standard-model fit to the Z^0 line shape, carried out by the ALEP II experiment [13].

It is a pleasure to thank the LEP Division for the smooth running of the accelerator and for continuing close cooperation with our experimental group. In addition to the support staff at our own institutions we are pleased to acknowledge the following: The Bundesministerium für Forschung und Technologie, FRG, The Department of Energy, USA, The Institut de Recherche Fondamentale du Commissariat à l'Energie Atomique, The Israeli Ministry of Science, The Minerva Gesellschaft, The National Science Foundation, USA, The Natural Sciences and Engineering Research Council, Canada, The Japanese Ministry of Education, Science and Culture (the Monbusho) and a grant under the Monbusho International Science Research Program, The Science and Engineering Research Council, UK and The A. P. Sloan Foundation.

References

- [1] Y. Sakai *et al.*, to appear in *Proceedings of the XIV International Symposium on Lepton and Photon Interactions*, Stanford, California August 7-12, 1989, KEK Preprint 89-42. I. Adachi *et al.*, in same proceedings, KEK Preprint-89-31. K. Abe *et al.*, Phys. Rev. Lett 61 (1988) 915.
- [2] C. Albajar *et al.*, Phys. Lett. 185B (1987) 241.
- [3] H. Baer *et al.*, in *Physics at LEP*, V. 1, ed. J. Ellis and R. Peccei, CERN 86-02 (1986) p. 297.
- [4] S. Jadach and J. Kuhn, MPI-PAE/PTh 64/86.
- [5] D. Stoker *et al.*, Phys. Rev. D39 (1989) 1811.
- [6] F.A. Berends and R. Kleiss, Nucl. Phys. B178 (1981) 141; F.A. Berends, R. Kleiss and S. Jadach, Comp. Phys. Commun. 29 (1983) 185.
- [7] S. Jadach *et al.*, *KORALZ the Monte Carlo Program for τ and μ pair production processes at LEP/SLC*, unpublished (1989); S. Jadach *et al.*, *Z Physics at LEP 1*, CERN 89-08, ed. G. Altarelli *et al.*, vol. 1 (1989) 235.
- [8] M.Z. Akrawy *et al.*, Phys. Lett. 231B (1989) 530.
- [9] OPAL Technical proposal (1983) and CERN/LEPC/83-4.
- [10] M.Z. Akrawy *et al.*, submitted to Phys. Lett. B, CERN-EP/89-147.
- [11] T. Sjostrand, Comp. Phys. Comm. 39 (1986) 345; JETSET, Version 7.1.
- [12] J.A.M. Vermaseren, Nuc. Phys. 229B (1983) 347.
- [13] D. Decamp *et al.*, CERN-EP/89-165.

Table 1: The expected total numbers of heavy lepton events produced at different center-of-mass energies for various heavy lepton masses; trigger and detection efficiencies are not included. The integrated luminosities shown have an uncertainty of $\approx 5\%$.

\sqrt{s} (GeV)	$\int L dt$ (nb $^{-1}$)	Heavy Lepton Mass (GeV/ c^2)										
		25	30	35	38	40	41	42	43	44	45	46
88.28	70.3	9.65	6.91	4.17	2.58	1.61	0.72	0.06	0.00	0.00	0.00	0.00
89.28	52.5	14.52	10.68	6.44	3.86	2.54	1.82	1.18	0.66	0.24	0.00	0.00
90.28	58.5	36.20	25.84	16.45	10.06	6.76	4.80	3.29	2.00	0.90	0.10	0.00
91.03	119.9	107.38	74.39	46.16	30.09	20.23	15.94	10.32	6.99	3.55	0.92	0.00
91.28	180.7	159.43	113.98	69.16	44.04	29.89	23.34	16.09	10.99	5.90	1.82	0.00
91.54	99.6	78.50	58.35	38.41	25.03	16.62	12.35	8.78	5.78	3.22	1.08	0.00
92.28	46.1	25.42	19.11	11.86	7.60	5.37	4.13	3.13	2.09	1.20	0.54	0.06
92.52	8.2	3.86	2.85	1.83	1.21	0.84	0.66	0.50	0.34	0.20	0.09	0.02
93.28	86.6	27.31	20.78	13.76	9.04	6.41	4.96	3.92	2.80	1.71	0.91	0.31
94.28	11.4	2.55	1.82	1.20	0.81	0.61	0.51	0.36	0.28	0.19	0.11	0.05
95.04	17.8	3.00	2.34	1.47	1.11	0.77	0.62	0.50	0.39	0.28	0.17	0.09
Total	751.60	467.8	337.0	210.9	135.4	91.6	69.9	48.1	32.3	17.4	5.7	0.5

Table 2: The numbers of events satisfying requirements at various stages in the analysis using E_{vis} and missing p_t . The data are given in the left column, and the Monte-Carlo calculation of different backgrounds are given in the next two columns. The two columns on the right give the number of events expected from a 42 GeV/ c^2 heavy lepton with massless ν_L (normalized to the integrated luminosity) and the efficiency for detecting this lepton at each stage in the analysis.

Requirements	Data	$Z^0 \rightarrow \tau\tau$	$Z^0 \rightarrow \text{hadrons}$	$Z^0 \rightarrow L^+L^-$	$\epsilon(L^+L^-)$
$p_t \geq 12, E_{vis} < 55, E_{FD} < 5$	315	204 ± 13	80 ± 15	24.5	0.51
Thrust ≤ 0.95	47	1 ± 1	24 ± 8	22.6	0.47
$E_{cone} < 1.0$ GeV	2	0	0 ± 2.7	21.2	0.44

Table 3: The numbers of events satisfying requirements at various stages in the isolated lepton analysis. The data are given in the left column. The two columns on the right give the number of events expected from a 42 GeV/c² heavy lepton with massless ν_L (normalized to the integrated luminosity) and the efficiency for detecting this lepton at each stage in the analysis.

Requirements	Data	L ⁺ L ⁻ (events)	L ⁺ L ⁻ (ϵ)
Isolated track	2063	18.0	0.37
Isolated lepton	1388	12.6	0.26
Not e^+e^- , $\mu^+\mu^-$, $\tau^+\tau^-$	84	12.4	0.26
No energy in FD	72	12.3	0.26
$E_2 > 2.0$ GeV	65	11.5	0.24
$p_t > 6$ GeV/c	20	11.0	0.23
$\theta_{acop} > 200$ mrad	1	10.0	0.21
Not $\ell^+\ell^-\gamma$	0	10.0	0.21

Table 4: The expected numbers of events satisfying selection requirements for various heavy lepton masses, summed over all center-of-mass energies. Column A gives these expected numbers for the missing energy and missing transverse momentum selection; column B gives the expected numbers for the isolated lepton selection; column C gives the numbers of events expected to satisfy either of these two selections. Entries in italics correspond to lepton masses not excluded by this analysis.

Mass (l^\pm) (GeV/c ²)	$m_{\nu_L} = 0$			$m_{\nu_L} = 0.50 m_L$			$m_{\nu_L} = 0.75 m_L$		
	A	B	C	A	B	C	A	B	C
10	10	37	46	5	26	32	0	<i>4.3</i>	<i>4.3</i>
20	127	64	174	64	44	100	4.5	8.5	13.0
30	124	62	151	89	38	113	10.3	11.4	21.4
40	36	17	44	33	11.2	39	4.2	4.8	8.4
42	21.1	10.1	24.1	18.0	6.3	20.8	<i>2.4</i>	<i>2.6</i>	<i>4.8</i>
43	14.1	6.8	16.2	12.2	4.6	14.4	<i>2.2</i>	<i>1.8</i>	<i>3.7</i>
44	7.6	3.7	8.7	7.1	2.6	8.2	<i>1.3</i>	<i>1.1</i>	<i>2.2</i>
45	<i>2.5</i>	<i>1.2</i>	<i>2.9</i>	<i>2.4</i>	<i>0.9</i>	<i>2.8</i>	<i>0.4</i>	<i>0.3</i>	<i>0.6</i>

Figure Captions

FIGURE 1: Distributions in visible energy(a) and missing transverse momentum(b) for a sample of hadronic Z^0 decays in the data(points) and for Monte Carlo(histogram).

FIGURE 2: Distribution in visible energy *vs* missing transverse momentum after requirements on thrust and cone energy for the data (a) and for a heavy lepton (b) of mass $42 \text{ GeV}/c^2$. The Monte-Carlo distribution is not normalized. The points lying near the search boundary are enlarged for clarity.

FIGURE 3: (a) Distributions in maximum transverse mass in events with an isolated lepton are compared for data and L^+L^- with $m_L = 42 \text{ GeV}/c^2$ and $\nu_L = 0$. (b) Distributions in θ_{acol} for isolated lepton data and the same L^+L^- events. In (b), the large number of entries in the last bin of the heavy lepton distribution corresponds to events where no energy is detected in the hemisphere opposite to the isolated lepton, in which case the acolinearity is defined to be π .

FIGURE 4: Distributions in missing transverse momentum *vs* acoplanarity for events with isolated leptons; all cuts except the last three in table 3 have been applied. Distributions for (a) the data and for (b) Monte-Carlo distributions from L^+L^- with $m_L = 42 \text{ GeV}/c^2$ and $\nu_L = 0$.

FIGURE 5: The 95% confidence level limits on m_L and $m_{\nu L}$ if ν_L is massive and stable. The limits of the excluded region are based on the combination of the missing p_t and isolated lepton searches; either search alone excludes most of this region. The sharp upper edge of the shaded region is defined by the lines $m_{\nu L} = m_L - 5 \text{ GeV}$ and $m_{\nu L} = 0.75m_L$.

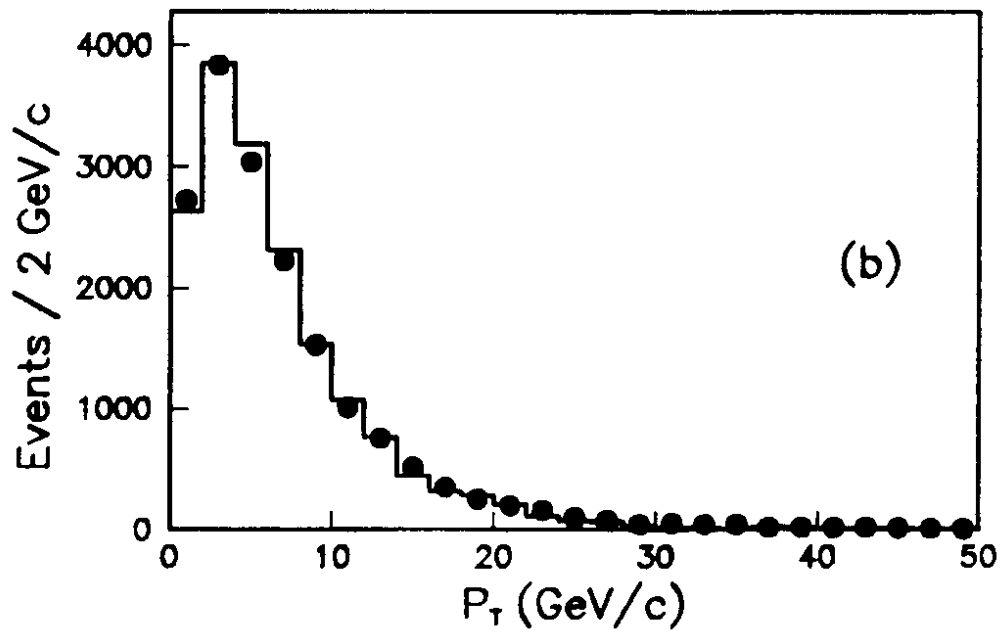
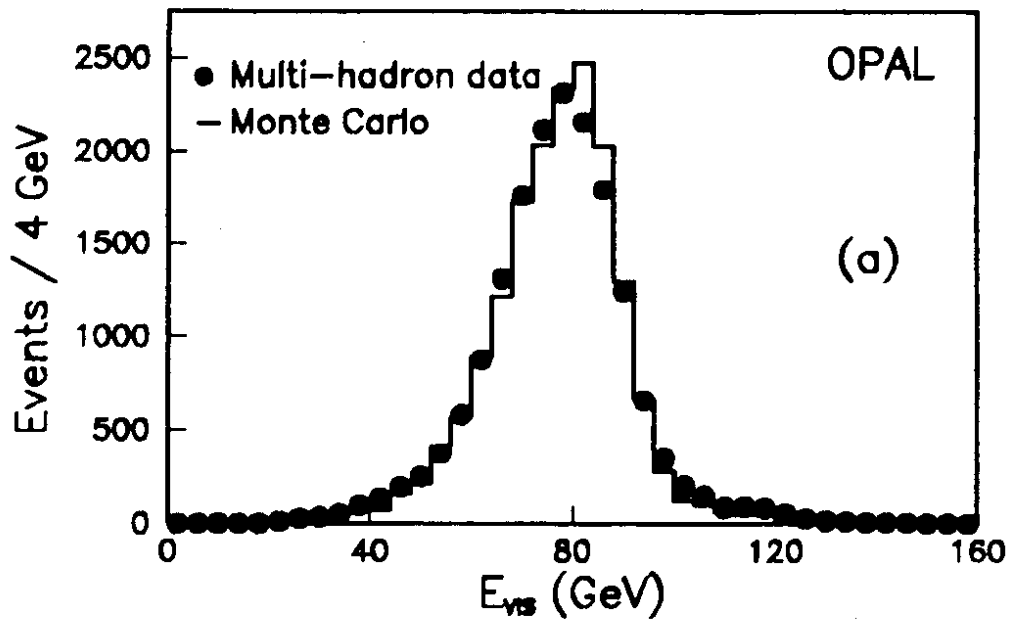


Figure 1

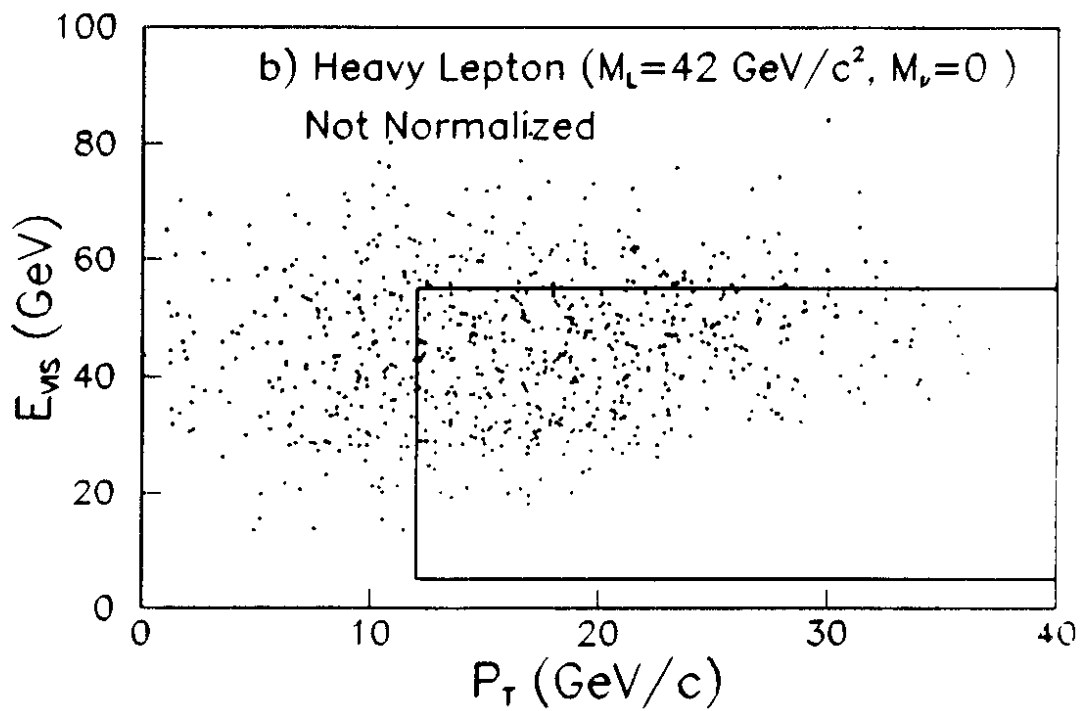
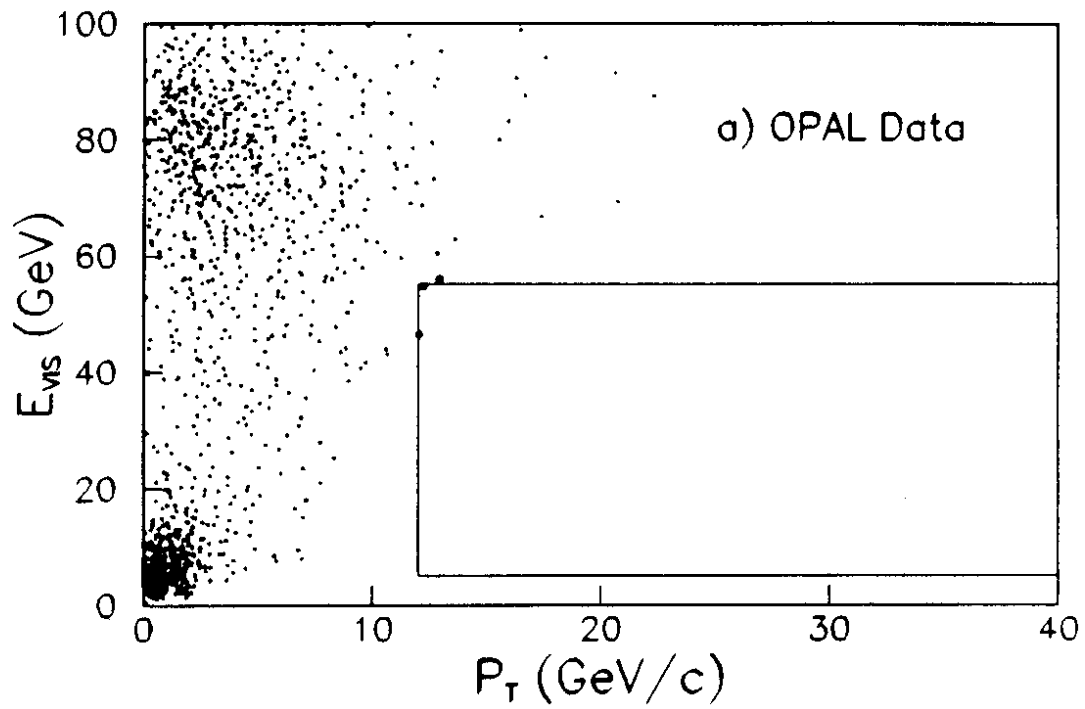


Figure 2

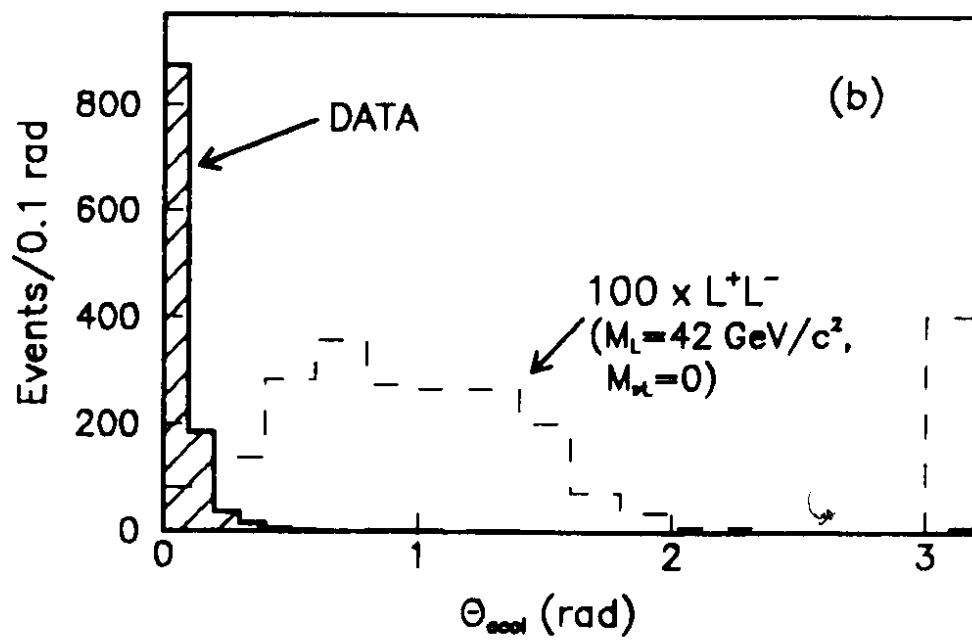
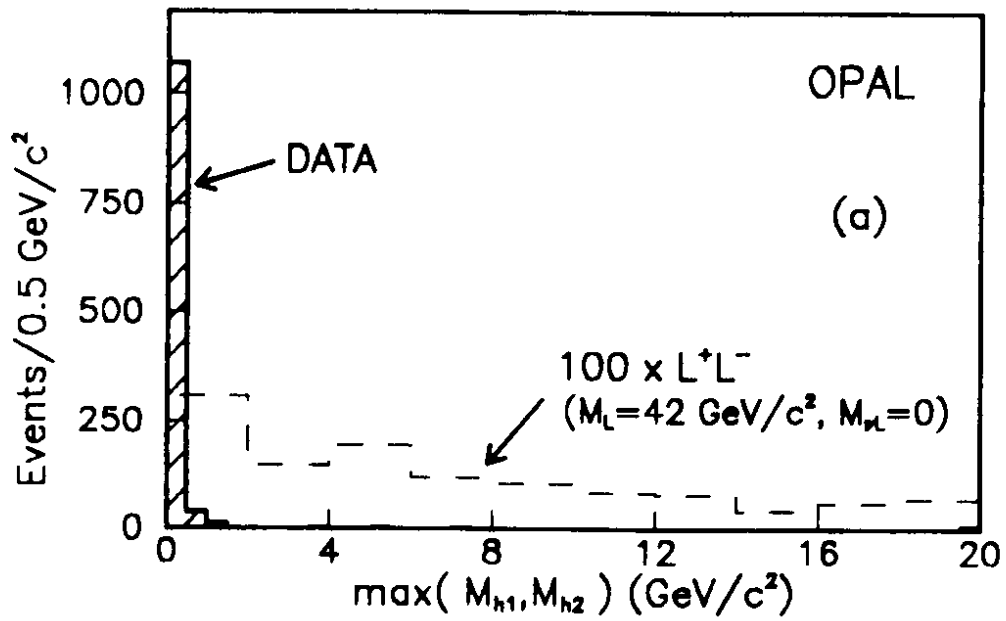


Figure 3

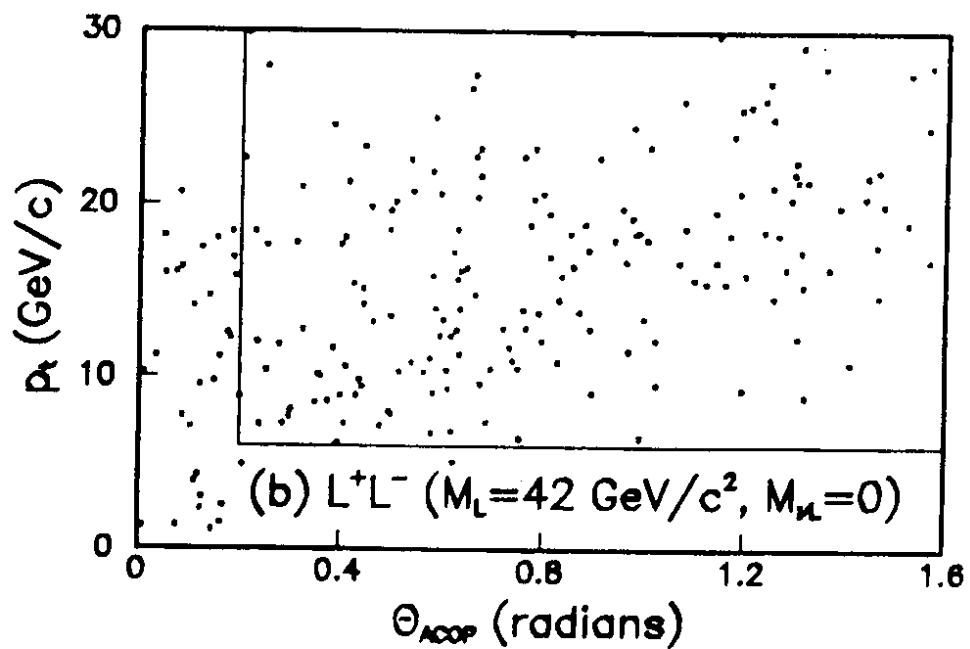
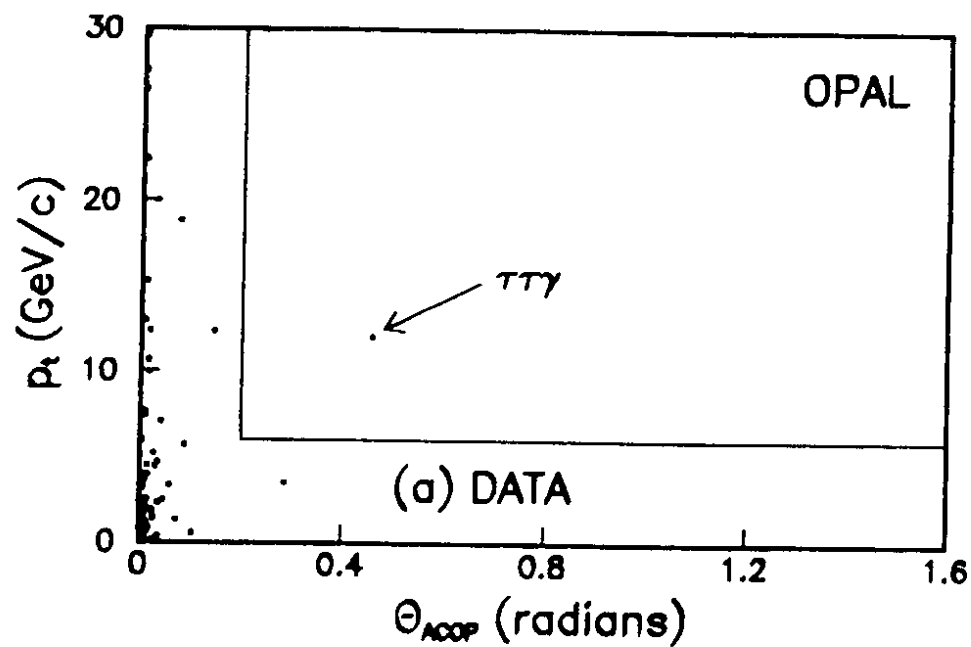


Figure 4

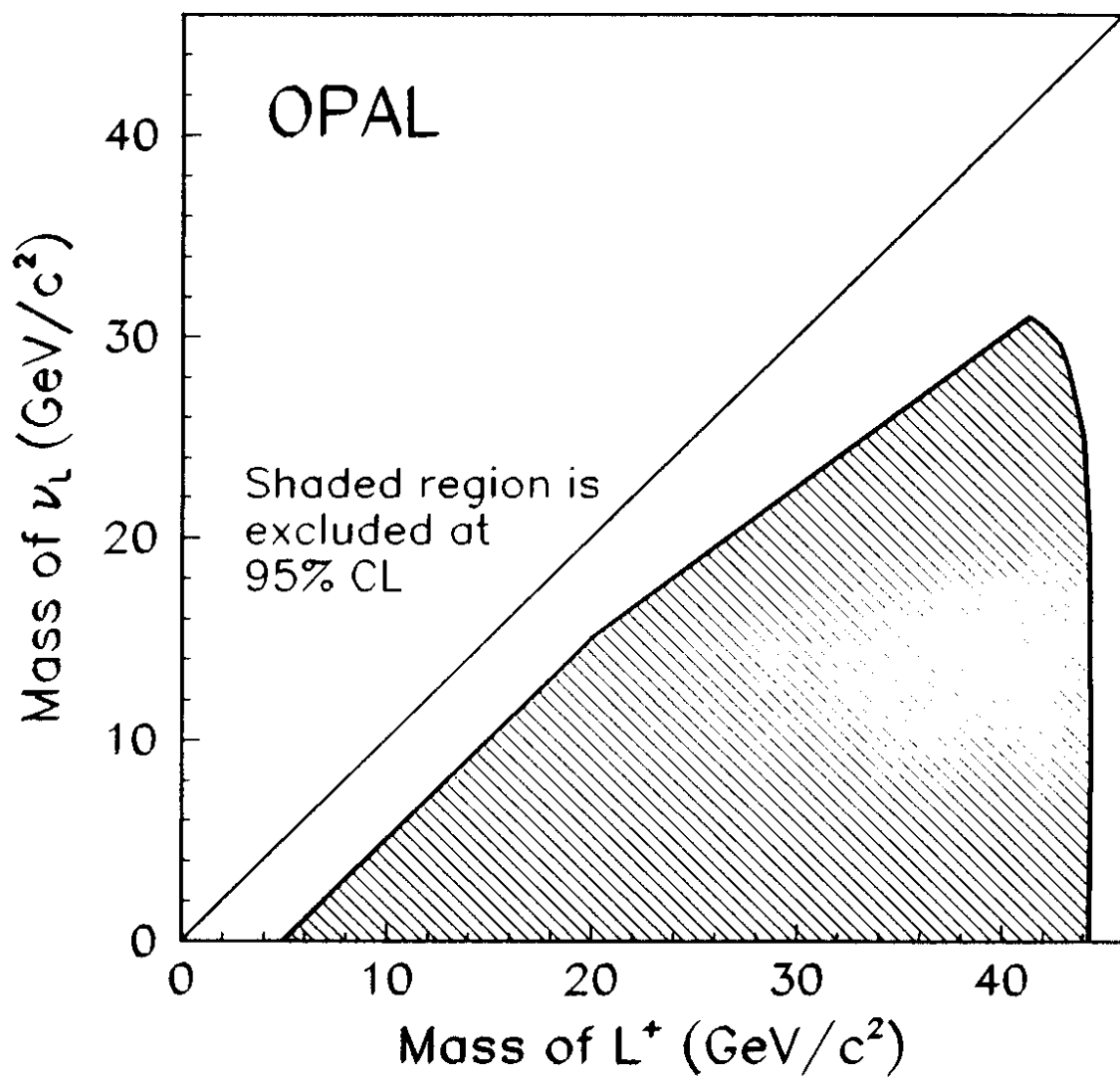


Figure 5